Research Article

Convoluted ν-Signals on ^{114}Cd Isotope from Astrophysical and Laboratory Neutrino Sources

Vaitsa Tsakstara[1,2]

^{1}*Technological Education Institute of Western Macedonia, 51100 Grevena, Greece*
^{2}*Division of Theoretical Physics, University of Ioannina, 45110 Ioannina, Greece*

Correspondence should be addressed to Vaitsa Tsakstara; vtsaksta@cc.uoi.gr

At first, we evaluate scattering cross sections of low, and intermediate-energy neutrinos scattered off the ^{114}Cd isotope, the most abundant Cd isotope present also in the COBRA detector (CdTe and CdZnTe materials) which aims to search for double beta decay events and neutrino observations at Gran Sasso laboratory (LNGS). The coherent ν-nucleus channel addressed here is the dominant reaction channel of the neutral current ν-nucleus scattering. Our ν-nucleus cross sections (calculated with a refinement of the quasiparticle random-phase approximation, QRPA) refer to the $gs \rightarrow gs$ transitions for ν-energies $\varepsilon_\nu \leq 100$ MeV. Subsequently, simulated ν-signals on ^{114}Cd isotope are derived. Towards this purpose, the required folded cross section comes out of simulation techniques by employing several low, and intermediate-energy neutrino distributions of the astrophysical ν-sources, like the solar, supernova, and Earth neutrinos, as well as the laboratory neutrinos, the reactor neutrinos, the pion-muon stopped neutrinos, and the β-beam neutrinos.

1. Introduction

In the past few decades neutrinos attracted a great part of the effort of the authors working in Nuclear, Astroparticle Physics and Cosmology [1–8]. Many neutrino experiments like the KamLAND [9], Borexino [10, 11], SNO+ [12], LENA [13], and other experiments, with high precision detectors aim to measure different types of neutrinos as well as neutrino-nucleus cross sections. Measurements in the beta-beam neutrino experiments [14–16] or in the expected to be built near spallation neutron sources (ORLAND experiment, Spallation Source) [17–20] may help answer key questions about the neutrino properties, the evolution of distant massive stars, the structure of the interior of our planet [21–23], and the fundamental electroweak interactions.

In recent terrestrial experiments aiming at neutrino studies through ν-nucleus interactions, the characteristics of the neutrino fluxes emitted by various neutrino sources like the astrophysical ν-sources (supernova, solar, and Earth neutrinos) or the laboratory ν-sources (accelerated β-decay ions in storage rings [15, 16], pion-muon decay at rest, e.g.,

at Fermilab [24], reactor neutrinos, etc.) are encoded on the nuclear response of the detector materials. On the theoretical side, the nuclear responses of ν-detectors to the energy spectra of the observed neutrino flux could be simulated by convoluted (folded) cross sections. The latter are obtained by using original ν-nucleus cross sections calculations and realistic descriptions for the ν-beam of the studied neutrino source [25–27], that is, reliable ν-energy distributions.

In the present paper, we study extensively the nuclear response to low and intermediate-energy neutrinos of the ^{114}Cd isotope focusing on the computation of flux averaged cross sections of this nucleus for various neutrino energy spectra. The Cd isotopes constitute significant materials of the semiconductors CdZnTe and CdTe detectors of the COBRA experiment which is aiming to search for double beta decay events and neutrino observations at Gran Sasso laboratory (LNGS) [4, 5, 12]. Calculation of the induced ν-signal in such nuclear detectors involves, first, evaluation of the flux of the neutrinos arriving at the detector and, second, folding of the calculated cross section of the neutrino interaction with the nuclear detector [6, 8]. The present

work is an extension of our previous studies which address inelastic cross sections of neutrinos scattered off the Te and Zn isotopes contents of the COBRA detector [6, 8, 28]. We pay special attention to the calculations of the elastic (coherent) neutral current (NC) neutrino-nucleus reaction cross sections for the ^{114}Cd nucleus (the most abundant isotope in the natural Cd). For similar calculations on other Cd isotopes the reader is referred to [29]. As it is well known, in NC ν-nucleus scattering the $gs \rightarrow gs$ transitions represent the dominant reaction channel [6, 30]. In terrestrial experiments the detection of this channel may be achieved through a measurement of the nuclear recoil signal [31–33] which is a rather different signature compared to that of the incoherent channel [1, 3, 6, 8, 34]. Inelastic scattering of neutrinos on nuclei creates different signal and could be studied through the outgoing charged-lepton and extracted nucleons and/or γ-ray emission. These channels have been studied in detail elsewhere (see, e.g., [6, 8, 30]).

For detectors of supernova neutrinos, all neutrino and antineutrino flavours take part in NC scattering on nuclear detectors (specifically heavy flavour neutrinos can be detected too) [4, 5, 35] while only electron-neutrino (ν_e) charged-current reactions are important (only a small portion of ν_x neutrinos has energy above the mass of the x-lepton which constitutes the main detection signal).

The solar neutrinos, which represent a powerful tool to investigate the Sun's deep interior [36, 37], have provided precious information to understand new physics and the interpretation of neutrino oscillations. Future experiments, like the SNO+ [12], are expected to contribute crucially in order to explore the CNO-cycle neutrino flux and clarify the open issue of the Sun's core metalicity.

Recently, geoneutrinos which are $\tilde{\nu}_e$ antineutrinos produced from decays of natural radioactive elements (predominantly ^{40}K and nuclides in the ^{238}U and ^{232}Th chains) mainly in the crust and mantle of the Earth have been successfully detected by the liquid-scintillator experiments of the KamLAND [38] and Borexino Collaborations [39], but the geological information contained in these measurements is still limited [40, 41]. Geoneutrinos are direct messengers of the abundance and matter distribution of radioactive elements deep within our planet, information that provides strong constraints on several phenomena occurring inside the Earth [42, 43]. Concerning the energy distribution of geoneutrinos, up to now little is known due to the fact that this is a new research field, but in the near future experiments like LENA, SNO+, and others, having in their objectives to explore geoneutrinos, are expected to provide us with new data. From the currently known information we imply that their energy range is $0 \leq \varepsilon_\nu \leq 10$ MeV.

It is expected [28] that the response of the Cd isotopes in the particle-bound excitation region, which coincides with the energy range of geoneutrinos, is rather rich and this motivates our present calculations. The next-generation detectors (LENA, Borexino, SNO) are expected to give useful answers to several questions of geological importance regarding the precise geo-ν fluxes and abundances of natural radioactive elements (K, U, and Th) in the Earth's interior [40–43].

One of the main goals of the present work is to focus on the interpretation of various ν-signals generated in nuclear detectors of terrestrial experiments through the investigation of the nuclear response of Cd detector medium to the corresponding neutrino energy spectra. We emphasize on signals coming from geo-, supernova-, solar-, reactor-, pion-muon stopped-neutrinos by using the following basic theoretical ingredients: (i) the calculated coherent total cross sections of the neutral-current reaction ^{114}Cd$(\nu, \nu')^{114}$Cd* computed with a refinement of the quasiparticle random-phase approximation (QRPA), (ii) reliable descriptions of the shapes of neutrino energy distributions provided mostly from numerical simulations of distributions of low energy neutrinos, and (iii) computational tools required for the folding procedure in order to simulate the signal expected to be recorded on Cd detectors as the CdTe or CdZnTe (the detector medium of COBRA experiment) from low-energy ν sources (geo-, reactor-, and solar-neutrinos) and intermediate-energy neutrinos (supernova and laboratory-neutrinos).

The paper is organized as follows. At first (Section 2) the main formalism is described and our cross section calculations are presented. Then, (Section 3), a description of the main characteristics of the low- and intermediate-energy neutrino sources addressed here is briefly summarized and folded cross sections as well as event rates for neutral current neutrino scattering off the ^{114}Cd isotope are discussed. Finally (Section 4), the main conclusions of the present work are extracted.

2. Brief Description of the Formalism

2.1. Angle Differential Coherent ν-Nucleus Cross Section. The angle differential cross section $d\sigma/d\Omega$ of the elastic scattering of a neutrino with energy ε_ν on a nucleus (A, Z) is [34, 44]

$$\frac{d\sigma}{d\Omega} = \frac{G_F^2}{4\pi^2} \varepsilon_\nu^2 \left(1 + \cos\vartheta\right) \frac{Q_w^2}{4} \mathscr{F}\left(q^2\right)^2, \tag{1}$$

where G_F is the Fermi coupling constant and $\mathscr{F}(q^2)$ contains the nuclear dependence of the cross section given by

$$\mathscr{F}\left(q^2\right) = \frac{1}{Q_w} \left[N F_N\left(q^2\right) + \left(1 - 4\sin^2\vartheta_W\right) Z F_Z\left(q^2\right) \right]. \tag{2}$$

In (1), ϑ represent the scattering angle and Q_w denotes the weak charge of the target nucleus:

$$Q_w = N + \left(1 - 4\sin^2\vartheta_W\right) Z, \tag{3}$$

(the weak mixing angle is $\sin^2\vartheta_W \approx 0.231$ [45]).

The ground state elastic nuclear form factors $F_Z(q^2)$ for protons and $F_N(q^2)$ for neutrons are defined by

$$F_k\left(q^2\right) = \frac{k}{4\pi} \int j_0\left(qr\right) \rho_{n,p}\left(r\right) d^3r, \quad k = N, Z \tag{4}$$

and are normalized as $F_{N,Z}(q^2 = 0) = 1$. In (4), $\rho_{n,p}(r)$ denote the neutron (n) and proton (p) charge density distribution

with $j_0(qr) = \sin(qr)/(qr)$ being the zero-order spherical Bessel function (we neglect a small correction from the single-nucleon form factors). The proton density $\rho_p(r)$ is often taken from experiment whenever measured charge densities are available [44, 46]. Moreover, some authors assume $F_N \approx F_Z$. From (1) we can easily obtain the expression with respect to the scattering angle ϑ as

$$\frac{d\sigma(\varepsilon_\nu, \vartheta)}{d\cos\vartheta} = \frac{G_F^2}{8\pi}(1 + \cos\vartheta)\,\varepsilon_\nu^2$$
$$\cdot\left[f_V^p Z F_Z\left(q^2\right) + f_V^n N F_N\left(q^2\right)\right]^2, \tag{5}$$

where f_V^p and f_V^n stand for the polar-vector coupling for the weak neutral current for proton and neutron, respectively, given by:

$$f_V^p = -\frac{1 - 4\sin^2\vartheta_W}{2}, \qquad f_V^n = -\frac{1}{2}. \tag{6}$$

From the latter two equations one can imply that the consideration of $F_N(q^2)$ in the cross section is important especially for heavier ν-detection targets. Thus, the coherent cross section depends on the square of the ground state nuclear form factor $\mathcal{F}(q^2)$ at momentum transfer q^2 which (in the extreme-relativistic limit) is given by

$$q^2 = 2\varepsilon_\nu^2(1 - \cos\vartheta), \tag{7}$$

or $q = 2\varepsilon_\nu \sin(\vartheta/2)$.

From (2), we see that, since $(1 - 4\sin^2\vartheta_W \approx 0.04)$ is small, a neutrino scattered elastically on a spin-zero nucleus couples mostly to the neutron distribution, $\rho_n(r)$. A measurement of the cross section for this process would, at some level, provide a determination of the neutron form factor $F_N(q^2)$. Some authors consider that this would be complementary to parity violating experiments because it would provide additional data, obtained at different energy ranges and with different nuclei that could be used to calibrate nuclear structure calculations [34, 44, 46–48].

2.2. Coherent Differential Cross Section with respect to Nuclear Recoil Energy T_A.

From an experimental point of view and particularly for the neutrino facilities near spallation sources [18, 33] the expression of the coherent differential cross section with respect to the nuclear recoil energy T_A is also interesting. This is written as [31–33, 49]

$$\frac{d\sigma(\varepsilon_\nu, T_A)}{dT_A} = \frac{G_F^2}{4\pi}Q_W^2 M\left(1 - \frac{MT_A}{2\varepsilon_\nu^2}\right)F\left(2MT_A^2\right), \tag{8}$$

where M is the nuclear mass and F denotes the ground state elastic form factor. More accurate expressions, including higher order terms with respect to T_A, can be found in [31–33, 50]. It should be noted that the signal on the coherent neutrino-nucleus scattering experiments is significantly different to that of the incoherent scattering where the signal could be an outgoing particle.

2.3. Total Coherent Cross Section.

The total coherent cross section $\sigma_{\text{tot}}(\varepsilon_\nu)$ is obtained by integrating numerically Equation (5) over the angle ϑ ($\vartheta_{\min} = 0$ to $\vartheta_{\max} = \pi$) or (8) over T_A between

$$T_A^{\min} = \frac{T_A}{2} + \sqrt{\frac{T_A}{2}\left(M_A + \frac{T_A}{2}\right)} \tag{9}$$

to $T_A^{\max} = \infty$ [50]. Some authors [48], however, ignoring the momentum dependence of the nuclear form factors take $F_N(q^2) \approx F_Z(q^2) \approx 1$ and in this case the total coherent cross section $\sigma_{\text{tot}}(\varepsilon_\nu)$ is approximately written as

$$\sigma_{\text{tot}}(\varepsilon_\nu) = \frac{G_F^2}{8\pi}[Z(4\sin^2\vartheta_W - 1) + N]^2\varepsilon_\nu^2. \tag{10}$$

Also, because $4\sin^2\vartheta_W - 1 \ll 1$ many authors take $\sigma_{\text{tot}} \propto N^2\varepsilon_\nu^2$ [48].

3. Results and Discussion

3.1. Original Cross Section Calculations.

The neutral-current scattering of low- and intermediate-energy neutrinos, ν_l, and antineutrinos, $\tilde{\nu}_l$, off the most abundant Cd isotope of the COBRA detectors, that is, the ^{114}Cd isotope (with abundance 28.8%), the main subject of our present work, is represented by the reactions

$$\nu_l\left(\tilde{\nu}_l\right) + {}^{114}\text{Cd} \longrightarrow {}^{114}\text{Cd}^* + \nu_l'\left(\tilde{\nu}_l'\right), \tag{11}$$

($\ell = e, \mu, \tau$ and ^{114}Cd* denotes an excited state of ^{114}Cd isotope). We mention that the above reactions (also the CC reactions for $\ell = e$) play significant role in astrophysical environment since they affect the electron fraction Y_e of the stellar matter [21–23].

In the first stage of the present work, we evaluate original cross sections for the reactions of (11). These calculations refer to the coherent channel (ground state to ground state transitions) of the target nucleus ^{114}Cd [1, 6, 8, 51–53]. As can be seen from (5) the original cross section identically comes for scattering of neutrinos ν_l and antineutrinos $\tilde{\nu}_l$. However, as we will see in Section 3, the signal on the nuclear detector could be significantly different due to the different ν-energy distributions.

In this work, we use theoretical densities obtained from simple mean-field calculations using the successful Woods-Saxon effective interaction plus the monopole (pairing) Bonn C-D interaction.

The ground state $|J_i^{\pi_i}\rangle = |0^+\rangle$ of the studied (even-even) ^{114}Cd isotope is computed by solving iteratively the BCS equations. In Table 1, we list the values of the pairing parameters ($g_{\text{pair}}^{p,n}$) and the theoretical energy gaps ($\Delta_{p,n}^{\text{th}}$) for protons (p) and neutrons (n) determined at the BCS level for the ^{114}Cd isotope. These parameters renormalise the pairing force and adjust the gaps $\Delta_{p,n}^{\text{th}}$ to the empirical ones $\Delta_{p,n}^{\text{exp}}$ obtained through the application of the three-point formulae (see [8]). The values of the $g_{\text{pair}}^{p,n}$ that adjust the energy gaps in both cases are reliable (see Table 1).

TABLE 1: Parameters determining the BCS ground state pairing interactions for protons (g_{pair}^P) and neutrons (g_{pair}^n) and the relevant theoretical values of proton (Δ_p^{th}) and neutron (Δ_n^{th}) energy gaps. The latter reproduce well the corresponding (for ^{114}Cd isotope) empirical energy gaps, $\Delta_{p,n}^{exp}$, listed also in the table, obtained through the three-point formula [6]. The values of the harmonic oscillator size parameter b, used for ^{114}Cd isotope, are also shown.

Isotope	Z, N	Abundance (%)	b (fm)	g_{pair}^n	g_{pair}^P	Δ_p^{exp}	Δ_p^{th}	Δ_n^{exp}	Δ_n^{th}
^{114}Cd	48, 66	28.73	2.214	0.9564	0.9753	1.441	1.44108	1.351	1.35093

Afterwards, the proton and neutron nuclear form factors are obtained from the expression

$$F_k\left(q^2\right) = \frac{1}{k}\sum_j \hat{j}\left\langle(n\ell)\,j\right| j_0\left(qr\right)\left|(n\ell)\,j\right\rangle\left(V_j^k\right)^2, \quad k = N, Z, \tag{12}$$

where V_j^k is the single particle $(n\ell)\,j$-level occupation probability amplitude for protons or neutrons (the summation runs over the 15 active levels of the model space chosen which consists of the major harmonic oscillator shell with quantum number $N = 3, 4, 5$) as well as over the fully occupied core j-levels having $V_j^k = 1$.

In Figure 1, we show the ingredients required for (1) and (5) in order to calculate the differential and integrated coherent cross section for the neutrino reactions of (11). Figure 1(a) shows the theoretical form factors for protons (F_Z) and neutrons (F_N) obtained with our BCS calculations and Figure 2 shows the momentum dependence of $F_{N,Z}(q^2)$ that enters (1) and (5). In this figure, the results obtained by assuming zero momentum transfer ($q \approx 0$), that is, $F_Z(q^2) = F_N(q^2) = \mathscr{F}(q^2) = 1$, are also presented (dash dotted curve). We see that, for energies above about 40 MeV, the two methods give significantly different results; the approximation $F_Z = F_N = \mathscr{F} = 1$ is good only for small momentum transfer (e.g., solar and low-energy SN-neutrinos). This shows also the sensitivity of the total cross sections of the total cross sections on the nuclear form factor.

Figure 2 illustrates the coherent cross sections of ν-^{114}Cd scattering as a function of (i) the momentum transfer q (Figure 2(a)) and (ii) the incoming neutrino energy ε_ν (Figure 2(b)). The original cross sections will be used below for evaluations of flux averaged folded cross sections for various neutrino sources. Towards this purpose, the ν-energy distributions of each source are required. We mention that here we have neglected the threshold energy of the detector (calculations where the threshold energy is considered have been performed in [54]).

In the next subsection, we summarize the main features of the neutrino energy distributions adopted in this work.

3.2. Energy Spectra of Low- and Intermediate-Energy ν-Sources.
The real neutrino sources, astrophysical (solar, supernova, and geoneutrinos) and laboratory (β-beam, pion-muon stopped neutrino beams, and reactor neutrinos), with few exceptions such as the ν_μ neutrino beam emerging from the π^+ decay at rest ($\varepsilon_\nu = 29.8$ MeV), the ^{7}Be solar neutrinos ($\varepsilon_\nu = 0.862$ MeV [10, 11]), and so forth, produce neutrinos that present a spectral distribution, characteristic of the

source itself (i.e., on the reactions producing the considered neutrinos), and are defined by

$$\frac{dN_\nu\left(\varepsilon_\nu\right)}{d\varepsilon_\nu} \equiv \eta\left(\varepsilon_\nu\right), \tag{13}$$

N_ν denotes the number of neutrinos of the beam. Thus, for example, the ν_e neutrinos originating from pion-muon decay at rest have energy spectra approximately described by the well-known Michel distribution, while the supernova neutrinos are commonly interpreted by using for their energy spectra a two-parameter Fermi-Dirac or power law distributions [6, 8, 28] (see below).

In this section, we summarize briefly the basic features of the currently interesting low-energy astrophysical and laboratory neutrino sources: solar, supernova, geoneutrinos, reactor neutrinos, pion-muon stopped neutrinos, and β-beam neutrinos. We focus on their energy distributions which drop in the neutrino energy range of our original cross sections. These neutrino spectra will be used in the folding procedure in the next section, in order to simulate the nuclear detector response of the ^{114}Cd nucleus and calculate event rates.

3.2.1. Geoneutrinos.
Geoneutrinos (or Earth neutrinos) are mainly electron antineutrinos ($\widetilde{\nu}_e$) generated upon transmutation of neutron-rich β-decay nuclei, accompanied by emission of an electron (e^-) and release of decay energy (Q_β) according to the reaction [40]

$$(A, Z) \longrightarrow (A, Z + 1) + e^- + \widetilde{\nu}_e + Q_\beta. \tag{14}$$
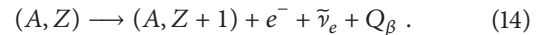
In the latter reaction A is the mass number and Z the atomic (proton) number of the initial (parent) nucleus. Part of the decay energy, $Q_\beta = Q_\nu + Q_h$, is carried away by antineutrinos (Q_ν) while the remainder is available for heating (Q_h). KamLAND is the first detector to conduct an investigation on geoneutrinos [40]. As it is well known, cosmochemical analysis expects significant amount of radioactive isotopes contained in the Earth and radiogenic heat generation of which totals up to about 20 TW [41].

The abundant radioactive isotopes that are in the present Earth are classified into three groups: (i) isotopes in the ^{238}U decay series, (ii) isotopes in ^{232}Th decay series, and ^{40}K isotope. These isotopes are the geologically important isotopes that heat the Earth's interior (they finally decay into stable nuclei). Radiogenic heat is produced by decays of isotopes, in which electron-type (anti-) neutrinos are emitted.

Figure 3(a) shows the antineutrino spectra from ^{40}K, ^{238}U series, and ^{232}Th series ($\tau_{1/2} = 4.47 \times 10^9$ year, $\tau_{1/2} = 14.0 \times 10^9$
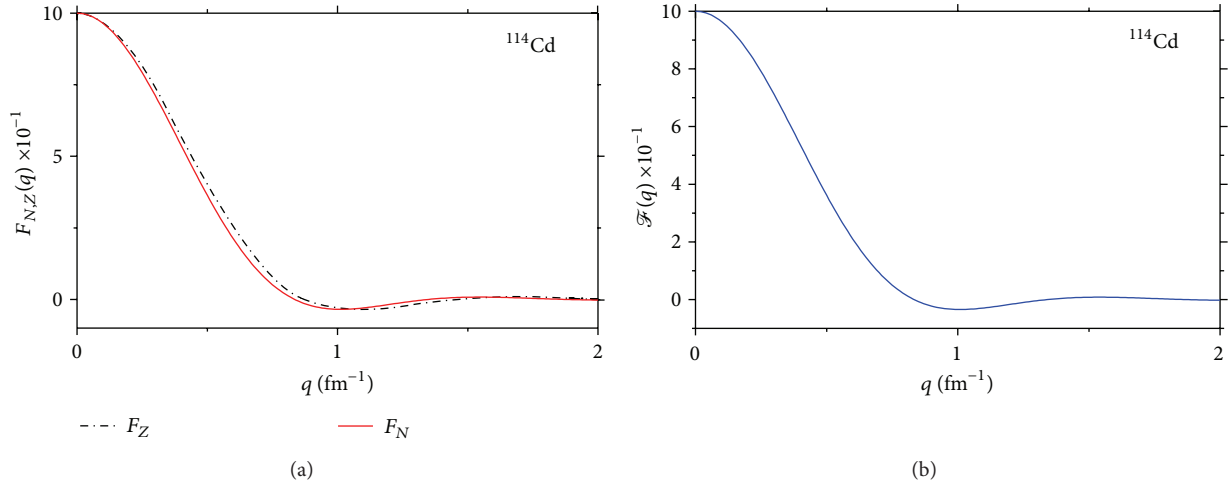
Figure 1: (a) Form factor $\mathscr{F}_{N,Z}(q^2)$ (for neutrons and protons) for ^{114}Cd isotope. (b) The ground state elastic nuclear form factor $F(q^2)$.
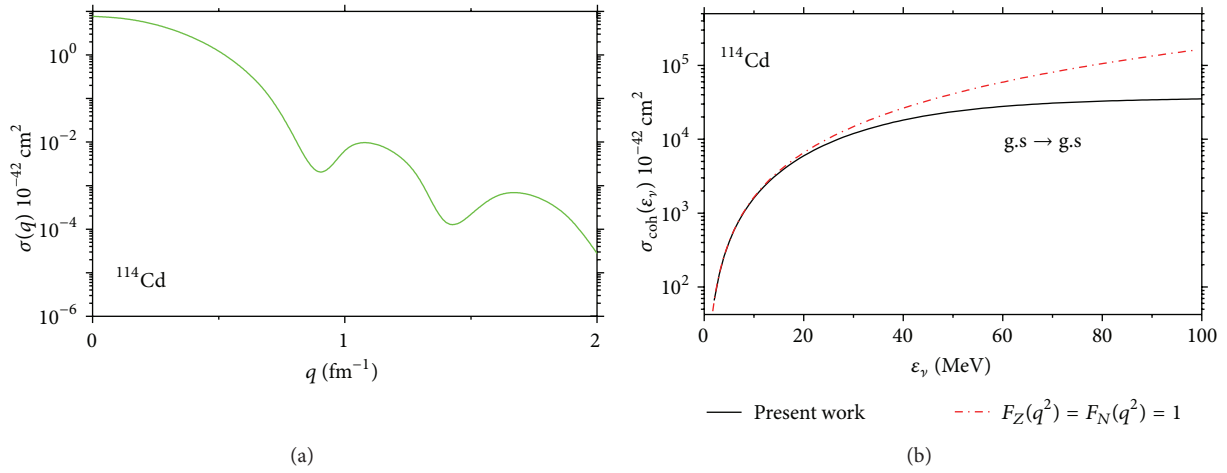
Figure 2: Coherent total cross section for the neutral current reactions ^{114}Cd$(\nu_l, \nu'_l)^{114}$Cd*, $l = e, \mu, \tau$: (a) as a function of the momentum transfer q and (b) as a function of the incoming neutrino energy ε_ν. The dash dotted curve results by assuming zero momentum transfer; that is, $F_Z(q^2) = F_N(q^2) = \mathscr{F}(q^2) = 1$.

year, and $\tau_{1/2} = 1.28 \times 10^9$ year, resp.). In this neutrino energy distribution $\tilde{\nu}_e$, coming from 82 beta decays in the U series and 70 beta decays in the Th series, are included. Antineutrinos are generated by β-decays of all intermediate radioactive isotopes [40–43].

The most recent measurements from KamLAND [38] and Borexino [39] are reaching the precision where they can start to constrain Earth models. However, these detectors are not sensitive to the neutrino direction. The amount of heat-producing elements in the Earth's mantle is of great interest and hence a detector located away from neutrinos produced in continental crust or on the ocean would be ideal [55]. The next-generation liquid-scintillator neutrino observatory, LENA [13], thanks to its large volume, would be a real breakthrough in geoneutrino detection and geologically significant results could be obtained. LENA could measure the total geoneutrino flux at the level of few percent, by far more precise than other current experiments (e.g., Borexino

or KamLAND) could reach. The event and background rates expected for LENA (both in Pyhäsalmi and Fríejus), and projects the precision at which the total geoneutrino flux as well as the U/Th ratio could be measured [13]. The large number of events expected for geoneutrinos will give valuable information on the abundances of Uranium and Thorium and their relative ratio in the Earths crust and mantle.

3.2.2. Reactor Neutrinos. Nuclear reactors have been used as intense ν_e sources in many experiments. In the fission of ^{235}U, ^{239}Pu, and ^{238}U, neutron-rich nuclei are produced and $\tilde{\nu}_e$ antineutrinos are subsequently emitted via β-decay [56, 57]. Experiments using reactor neutrinos are particularly suitable for low Δm measurement because the mean energy of the reactor neutrinos is a few MeV (much smaller than that of accelerator neutrinos). The distance from the reactor core in many reactor experiments is ranged from several tens of meters to 1 km while the overall systematic errors

(a)

(b)
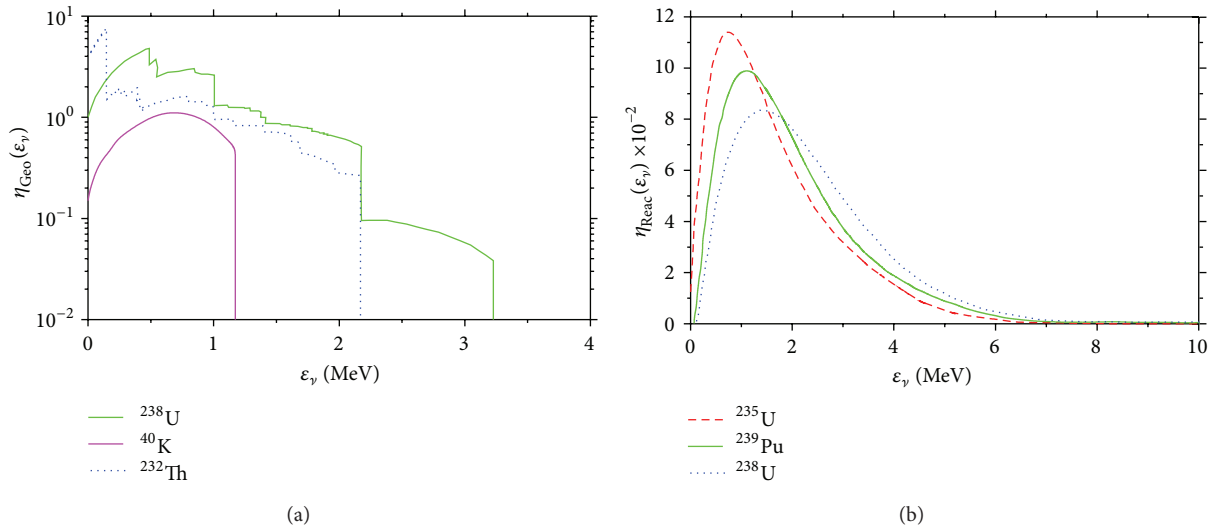
FIGURE 3: (a) Spectra of the U Series, Th Series, and ^{40}K geoneutrinos. Neutrinos from ^{40}K electron capture are also shown in this figure. (b) Normalized reactor neutrino spectra.

including the ν_e flux uncertainty and detector uncertainty are constrained to within a few % at these experiments.

Nuclear reactors, as sources of $\tilde{\nu}_e$, give fluxes of the order $\sim 10^{13}$ $\tilde{\nu}/cm^2$ sec at distances ~ 10 m from the reactor core. These antineutrinos have an energy spectrum peaked at very low energies (~ 0.3 MeV) and extending up to ~ 10 MeV, characteristic of the β^- decay of the fission products. Figure 3(b) illustrates the reactor neutrino spectra normalized so that the sum over all data-points is equal to one. The fuel composition was adopted to be 62% ^{235}U, 30% ^{239}Pu, and 8% ^{238}U [56, 58].

3.2.3. Solar Neutrinos.

Solar neutrinos are ν_e neutrinos produced through weak, electromagnetic, and strong nuclear processes in the interior of our Sun. They have energy $\varepsilon_\nu \leq 18$ MeV and are created either via the well-studied pp-chain reactions or via the CNO-cycle processes [36]. Their energy depends not only on the pertinent nuclear processes, but also on the densities and temperatures in the Sun's environment. The detection of solar neutrinos by terrestrial experiments provides unique information about the interior of the Sun and constitutes excellent probes for astrophysics, nuclear physics, and particle physics searches.

In Figure 4(a), we show the energy spectra of the important ^{8}B and hep neutrino sources predicted by the standard solar model. Each of these spectra has a characteristic shape which is independent of the conditions in the solar interior. The ^{8}B spectrum, on the other hand, is more nearly symmetric, with a peak at 6.4 MeV and a somewhat extended tail. The hep spectrum is rather symmetric and peaks at 9.6 MeV. We mention that measurements of the spectrum of neutrinos that reaches us from the sun provided a decisive test of whether the solar neutrino puzzle is due to our lack of understanding of the solar interior or due to new physics [36, 37].

3.2.4. Pion-Muon Decay at Rest Neutrino Energy Distributions.

In the operating pion-muon decay at rest neutrino sources (Fermilab at USA, J-PARC at Japan) and the expected to operate neutrino facilities at the Neutron Spallation Sources (ORNL at USA, and Lund in Sweden), ν_e neutrinos and $\tilde{\nu}_\mu$ antineutrinos are produced from the decay of muons according to the reaction

$$\mu^+ \longrightarrow e^+ + \nu_e + \tilde{\nu}_\mu. \tag{15}$$

The decaying muons result from the decay of slow pions ($\pi^+ \rightarrow \mu^+ + \nu_\mu$) and hence, ν_e and $\tilde{\nu}_\mu$ neutrinos have relatively low energies. Their energy spectra are approximately described by normalized distributions of the form [2, 59]

$$\eta_{\nu_e}(\varepsilon_\nu) = 96\varepsilon_\nu^2 M_\mu^{-4} \quad \left(M_\mu - 2\varepsilon_\nu\right), \tag{16}$$

$$\eta_{\tilde{\nu}_\mu}(\varepsilon_\nu) = 16\varepsilon_\nu^2 M_\mu^{-4} \quad \left(3M_\mu - 4\varepsilon_\nu\right), \tag{17}$$

where $M_\mu = 105.6$ MeV is the muon rest mass (see Figure 4(b)). The maximum energy of ν_e and $\tilde{\nu}_\mu$ in the later equations is $\varepsilon_\nu^{max} = 52.8$ MeV $= M_\mu/2$ [59, 60]. The distribution of these ν_e neutrinos is known as Michel energy spectrum. The pion-muon decay at rest neutrino beams is not completely pure as, for example, the β-beam neutrinos.

Obviously, the analytic expressions of (16) and (17) are convenient for the required numerical integration in the folding procedure [6, 8, 28, 61–63]. Their energy range and shape roughly resemble those of supernova neutrinos and give us a unique opportunity to study neutrino interactions in this important energy range. This will improve our understanding of SN dynamics and help us to design and calibrate the response of supernova neutrino detectors. We should mention, however, that the pion-muon decay at rest neutrino distributions is closed for high energies while the SN neutrino spectra are open at their high energy tail (see below).
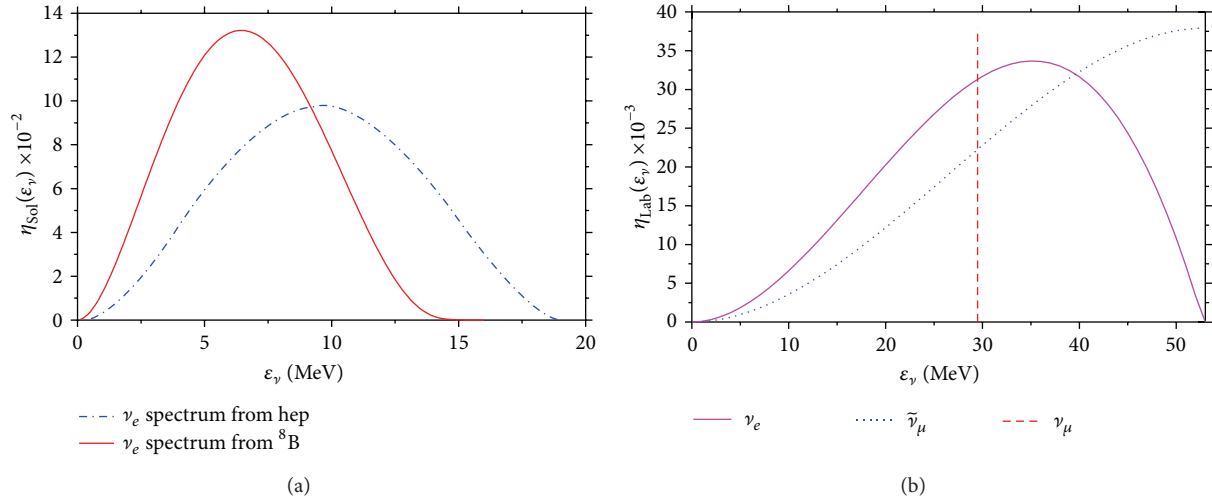
FIGURE 4: (a) Normalized energy spectrum of ^{8}B and hep ν_e solar neutrinos. (b) Energy spectra of ν_e and $\widetilde{\nu}_\mu$ neutrino beams, generated from the muon-decay at rest.

3.2.5. Supernova Neutrinos. According to predictions of recent numerical simulations [64, 65], the creation of the supernova neutrino fluxes is a very complicated process. The shape of SN-neutrino energy distributions is determined by the conditions under which the neutrinos are emitted from the star causing the cooling of the protoneutron star formed at the center of the collapsing star [21, 66–69]. In earlier studies, a thermal spectrum was employed to describe the SN-ν energy distribution [70]. Recent stellar evolution simulations, however, have shown that several effects modify the spectral shape from a purely thermal one [64].

In stellar modelling, authors use analytic expressions that include various modulation effects by inserting a chemical potential μ. Such an expression is as the well-known two-parameter Fermi-Dirac (FD) distribution [64]. A similar expression is the analytically simpler two-parameter Power-Law (PL) energy distribution [64, 65, 71]. Both parametrizations FD and PL yield similar distributions characterized by the temperature T or the average ν-energy $\langle\varepsilon_\nu\rangle$ [8, 28, 72–74]. It is important to note that the flavour-dependent fluxes and spectra emitted by supernovae at any distance from the source can be different from those originally produced, which is mainly due to neutrino oscillations but also due to other phenomena [70].

In Figure 1 of [75, 76] some specific cases of Fermi-Dirac (FD) and Power-law (PL) distributions have been presented for various values of their parameters [64, 65]. Concerning the behaviour of FD and PL distributions throughout their energy range we mention the following features. For the Fermi-Dirac spectral distribution, as the temperature grows both the maximum of the PL distribution shifts to greater neutrino energy and its peak becomes smaller. Also, increasing the degeneracy parameter n_{dg} shifts the spectrum to higher energies [64, 65]. The Power-Law energy distribution is characterized by the pinching parameter α and average energy $\langle\varepsilon_\nu\rangle$. The average energy $\langle\varepsilon_\nu\rangle$ reflects the depth of the stars from where the neutrinos are escaping. As $\langle\varepsilon_\nu\rangle$ grows, the maximum of the distribution shifts to higher neutrino

energy ε_ν [65], while as the width parameter w [8] grows (for the same average energy $\langle\varepsilon_\nu\rangle$), both the maximum of the distribution shifts to smaller neutrino energy ε_ν and its peak becomes smaller. For the purposes of the present work, the values of the pinching parameter needed are α =5.1, 3.7, 2.7. The corresponding values of the parameters of $\langle\varepsilon_\nu\rangle$ are shown in Table 2.

It is important to note that the flavour-dependent fluxes and spectra emitted by an SN at any distance from the source can be different from those originally produced mainly due to neutrino oscillations in propagation and also due to other phenomena [70]. The high statistics of neutrino signal from a future galactic SN may allow us to unravel the relevant SN-neutrino scenarios.

The number of the emitted neutrinos can be obtained from the total emitted energy $U_\nu = 3\times10^{53}$ erg$N_\nu = U_\nu/\langle E_\nu\rangle$. The (time averaged) neutrino flux at a distance D from the source is $\Phi = N_\nu/(4\pi D^2)$ (for the SN 1987A $D = 10\,\mathrm{kpc} = 3.1\times10^{22}$ cm).

3.2.6. Low-Energy β-Beam Neutrinos. Recently, some accelerated β-radioactive nuclei have been proposed as sources of neutrino beams (beta-beam neutrinos) [14, 15, 77]. Such facilities may produce pure beam neutrinos in which the possible flavors are either the ν_e (for β^+-decaying ions) or the $\widetilde{\nu}_e$ (for β^--decaying ions) to search for standard and nonstandard neutrino physics at low and intermediate energies (ν-nucleus interactions, neutrino properties, neutrino oscillations, etc.) and measure ν-nucleus scattering cross sections [15, 77].

For the readers convenience, we summarize here the main features of the low-energy β-beam neutrinos. Their spectra [8, 75, 76] are characterised by the boost velocities (Lorentz factors or γ-factors). For most applications, we derive normalized synthetic neutrino energy distributions $\eta_{bb}(\varepsilon_\nu)$ given by linear combinations of the form

$$\eta_{bb}\left(\varepsilon_\nu\right) = \sum_{j=1}^{N}\alpha_j\eta_{\gamma_j}\left(\varepsilon_\nu\right), \tag{18}$$

TABLE 2: Flux averaged coherent cross sections $\langle\sigma_{\text{coh}}\rangle$ (in units 10^{-42} cm^2) for ^{114}Cd isotope obtained in the case of neutrino energy spectra coming from two neutrino sources: (i) supernova neutrinos and (ii) laboratory neutrinos.

Flux averaged cross sections $\langle\sigma_{\text{coh}}\rangle$ (10^{-42} cm^2)									
Supernova neutrinos								Neutrinos Pion-muon stopped	
Fermi-Dirac (FD)				Power Law (PL)				Michel spectrum	
$T =$	3.10	4.14	6.20	$\langle\varepsilon_\nu\rangle =$	12	16	24	$\eta_{\nu_e}(\varepsilon_\nu)$	$\eta_{\widetilde{\nu}_\mu}(\varepsilon_\nu)$
$\langle\sigma\rangle =$	2648	4457.52	8648.06	$\langle\sigma\rangle =$	2653.26	4452.93	8658.47	$\langle\sigma\rangle =$ 13109.52	15880.76

where N numbers the different Lorentz (γ) factors included in the synthetic spectrum (expressions for the individual distributions $\eta_{\gamma_j}(\varepsilon_\nu)$ are given in [7, 8, 74]). Combinations of the type $\eta_{bb}(\varepsilon_\nu)$ for γ-factors up to 10–12 are used to fit original supernova neutrino spectral distributions, $\eta_{\text{SN}}(\varepsilon_\nu)$, reaching terrestrial detectors by adjusting the weight parameters α_j through the minimization procedure described in [8, 75, 76].

Many authors in recent β-beam neutrino simulations employ the energy spectra of the antineutrinos $\widetilde{\nu}_e$ emitted from β^--radioactive $^6_2$He ions according to the reaction

$$^6_2\text{He} \longrightarrow {}^6_3\text{Li} + e^- + \widetilde{\nu}_e \qquad (19)$$
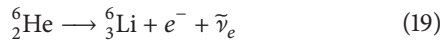
The Q-value of this reaction is $Q_{\text{He}} = 3.5$ MeV. Another potential β^--radioactive isotope for $\widetilde{\nu}_e$ beams is the $^8_3$Li with Q-value $Q_{\text{Li}} = 13.0$ MeV. Interesting β^+-radioactive ion source to be accelerated for producing ν_e beams is the $^{18}_{10}$Ne, which decays according to the reaction [15, 77]

$$^{18}_{10}\text{Ne} \longrightarrow {}^{18}_{9}\text{F} + e^+ + \nu_e \qquad (20)$$
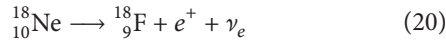
The Q-value of this reaction is $Q_{\text{Ne}} = 3.4$ MeV. For ν_e beams another promising β^+-radioactive isotope is the $^8_4$B ($Q_B = 13.9$ MeV).

From the aforementioned potential targets, $^6_2$He and $^{18}_{10}$Ne are considered to have rather low Q-values, so they are good choices for short baseline neutrino studies while $^8_3$Li and $^8_4$B have relatively high Q-values and they are the best choices for a large baseline [13].

Energy spectra of the reactions (19) and (20) for several integer γ-boost factors ($\gamma = 3, 4, \ldots, 15$) are discussed in [8, 74].

3.3. Simulated Neutrino Signals on Nuclear Detectors.
As mentioned in Section 1, the characteristics of the arriving at a nuclear detector neutrino flux are concealed in the nuclear response of the detector medium, that is, in the material CdTe or CdZnTe for the case of the COBRA detectors. Theoretically, these features could be simulated by convoluted cross sections calculations carried out as discussed in [64, 65, 71].

In the present work, the convolution (folding) method was performed with the original cross sections obtained as discussed before, in order to compute the flux averaged total cross sections, $\langle\sigma_{\text{tot}}\rangle$, for the low-energy neutrino spectra of the previous section.

For the coherent channel, which is possible only in neutral current neutrino-nucleus reactions studied in the present work, the flux averaged cross section $\langle\sigma_{\text{coh}}\rangle$ is defined as [2]

$$\langle\sigma_{\text{coh}}\rangle = \int_0^\infty \sigma_{\text{coh}}(\varepsilon_\nu)\,\eta(\varepsilon_\nu)\,d\varepsilon_\nu. \qquad (21)$$

Due to the dominance of the coherent cross section $\sigma_{\text{coh}}(\varepsilon_\nu)$ throughout the region of the incoming neutrino energy ε_ν, $\langle\sigma_{\text{coh}}\rangle$ is, sometimes, even two or three orders of magnitude larger than the incoherent one, $\langle\sigma_{\text{tot}}^{\text{incoh}}\rangle$ [6, 8, 28, 61].

The flux averaged cross sections obtained for ^{114}Cd with (21) for the neutrino distributions $\eta(\varepsilon_\nu)$ of Section 3 are listed in Tables 2 and 3. In Table 2 the flux averaged cross sections refer to various supernova neutrino scenarios described by the Fermi-Dirac (F-D) and Power-Low (P-L) distributions corresponding to the parameters given in this Table, that is, ν_e neutrinos, $\widetilde{\nu}_e$ antineutrinos, and ν_x, $x = \nu_\mu$, ν_τ, $\widetilde{\nu}_\mu$, and $\widetilde{\nu}_\tau$ [64, 65, 71]. In the last two columns of Table 2 we tabulate the $\langle\sigma_{\text{coh}}\rangle$ calculated for the distributions of (16) and (17). Here the flux averaged cross sections have been calculated as in [30].

In Table 3 we list the flux averaged cross sections evaluated by adopting the neutrino distributions of the geoneutrinos (see Figure 3(a)), of the reactor neutrinos (see Figure 3(b)) and solar neutrinos (see Figure 4(a)) for the ^{8}B-neutrinos and Figure 4(b) for the hep neutrinos).

3.4. Number of Events in nu-Detectors.
For another connection of the present theoretical results with the neutrino experiments discussed in Section 1, and specifically COBRA experiment, we estimate the signals created in the ^{114}Cd detector which is given by the expression [6, 78]

$$\sigma_{\text{sign}}(\varepsilon_\nu) = \sigma_{\text{coh}}(\varepsilon_\nu)\,\eta(\varepsilon_\nu). \qquad (22)$$

By using our theoretical cross sections $\sigma(\varepsilon_\nu)$ for ^{114}Cd isotope we may evaluate the neutrino fluxes Φ_ν or the scattering event rates, N_{event}, for the COBRA detector.

Our calculations here are based on a mass 100 Kgr of the COBRA detector with detector material CdZnTe or CdTe for the typical detection rate of $N_{\text{event}} = 1$ event hr^{-1}, t. Assuming that N_{Cd} is the total number of nuclei (atoms) of ^{114}Cd in the detector, we have [78]

$$\frac{dN_\nu}{dt} \equiv N_{\text{event}} = N_{\text{Cd}}\Phi_\nu(\varepsilon_\nu)\,\sigma_{\text{tot}}(\varepsilon_\nu). \qquad (23)$$

TABLE 3: Flux averaged coherent cross sections $\langle\sigma_{coh}\rangle$ (in units 10^{-40} cm^2) for ^{114}Cd isotope obtained in the case of neutrino energy spectra coming from two neutrino sources: (i) geoneutrinos, (ii) reactor neutrinos, and (iii) solar neutrinos.

Flux averaged cross sections $\langle\sigma_{coh}\rangle$ (10^{-42} cm^2)							
Detector ^{114}Cd	Geoneutrinos			Reactor neutrinos			Solar neutrinos	
	^{40}K	^{238}U	^{232}Th	^{235}U	^{238}U	^{239}Pu	^{8}B	hep
	151.38	1504.40	972.56	192.20	508.90	9604.36	8503.99	9956.57

TABLE 4: Neutrino coherent fluxes $\Phi_\nu(\varepsilon_\nu)$ (in units 10^9 sec^{-1} cm^2) for ^{114}Cd isotope for the two materials (CdTe and CdZnTe) of the COBRA experiment obtained in the case of supernova neutrinos with mean energies $\langle\varepsilon_\nu\rangle$ = 12, 16, and 24 MeV. N_0 is the Avogadro's number.

Neutrino coherent fluxes Φ_ν				
Detector medium	Number of atoms	^{114}Cd (Kgr)	$\langle\varepsilon_\nu\rangle$ (MeV)	Φ_ν ($\times 10^9$ sec^{-1} cm^{-2})
CdTe	$120.11N_0$	13.5	12	1.447
			16	0.862
			24	0.449
CdZnTe	$94.17N_0$	10.6	12	1.847
			16	1.100
			24	0.566

The COBRA detector is expected to have a total mass of ^{114}Cd CdZnTe about m_{Cd} = 10.6 Kgr which translates to about $N_{Cd} = N_{^{114}Cd} = 94.17N_{Avogadro}$ atoms (nuclei). The results from (23) neutrino fluxes for the supernova neutrinos with the mean energies $\langle\varepsilon_\nu\rangle$ = 12 MeV (electron neutrinos ν_e), $\langle\varepsilon_\nu\rangle$ = 16 MeV (electron anti-neutrinos $\tilde{\nu}_e$), and $\langle\varepsilon_\nu\rangle$ = 24 MeV ($\nu_x, \tilde{\nu}_x, x = \mu, \tau$) and the $\langle\sigma_{coh}\rangle$ of Table 2 are shown in Table 4 (first three lines).

Similar calculations will be done assuming that the material of COBRA detector is the CdTe. Again we consider 100 Kgr detector which contains 13.5 Kgr ^{114}Cd or about $N_{Cd} = N_{^{114}Cd} = 120.11N_{Avogadro}$ atoms (nuclei). The results from (23) neutrino flux for the supernova neutrino scenarios adopted above are shown in Table 4 (last three lines).

These results are encouraging for the Cd materials to be used in the future as astrophysical neutrino detectors in addition to their main goal of neutrinoless double β-decay search. We stress, however, that even though the above neutrino fluxes are of the same order with those expected at the Spallation Neutron Source at ORLaND, Oak Ridge [17–19], in choosing a neutrino cross section measurement target other experimental criteria usually lead to more popular choices (Xe, Cs, etc.). For such targets similar calculations to those we performed here for ^{114}Cd could be also done.

4. Conclusions

Astrophysical neutrinos (solar, supernova, and Earth neutrinos) are key particles in investigating the structure and evolution of stars, the astronuclear reactions, and also in deepening our knowledge on the fundamental interactions and the nuclear weak responses. In this work we applied the convolution procedure to calculate flux averaged cross sections and event rates for the above ν-sources based on neutrino-nucleus cross sections obtained with realistic

nuclear structure calculations (QRPA method). For the computed folded cross sections we employed specific spectral distributions describing neutrino-energy spectra of supernova and solar neutrinos, geoneutrinos, reactor neutrinos, laboratory neutrinos, and neutrinos produced from the decay of pions and muons at rest.

The flux-averaged total coherent cross sections, $\langle\sigma_{coh}\rangle$, reflect to some extent the neutrino signals generated in several selected terrestrial detectors from such ν-sources. In this work, we estimated coherent neutrino fluxes for ^{114}Cd which is content of the CdTe and CdZnTe materials of the COBRA detector at LNGS. The goal of this experiment is to search for double beta decay events and neutrino observation.

Conflict of Interests

The author declares that there is no conflict of interests regarding the publication of this paper.

Acknowledgments

References

[1] T. W. Donnelly and R. D. Peccei, "Neutral current effects in nuclei," *Physics Reports*, vol. 50, no. 1, pp. 1–85, 1979.

[2] T. S. Kosmas and E. Oset, "Charged current neutrino-nucleus reaction cross sections at intermediate energies," *Physical Review C: Nuclear Physics*, vol. 53, no. 3, pp. 1409–1415, 1996.

[3] H. Ejiri, "Nuclear spin isospin responses for low-energy neutrinos," *Physics Reports*, vol. 338, no. 3, pp. 265–351, 2000.

[4] K. Zuber, "COBRA—double beta decay searches using CdTe detectors," *Physics Letters B*, vol. 519, no. 1-2, pp. 1–7, 2001.

[5] K. Zuber, "Spectroscopy of low energy solar neutrinos using CdTe detectors," *Physics Letters B*, vol. 571, no. 3-4, pp. 148–154, 2003.

[6] V. Tsakstara and T. S. Kosmas, "Low-energy neutral-current neutrino scattering on ^{128,130}Te isotopes," *Physical Review C*, vol. 83, Article ID 054612, 2011.

[7] V. Tsakstara, T. S. Kosmas, and J. Wambach, "Studying low-energy astrophysical neutrinos with neutrino nucleus cross-section calculations and beta beam neutrino spectra," *Progress in Particle and Nuclear Physics*, vol. 66, no. 2, pp. 424–429, 2011.

[8] V. Tsakstara and T. S. Kosmas, "Analyzing astrophysical neutrino signals using realistic nuclear structure calculations and the convolution procedure," *Physical Review C*, vol. 84, Article ID 064620, 2011.

[9] S. Abe, T. Ebihara, S. Enomoto et al., "Precision measurement of neutrino oscillation parameters with KamLAND," *Physical Review Letters*, vol. 100, no. 22, Article ID 221803, 2008.

[10] G. Bellini, J. Benziger, S. Bonetti et al., "Observation of geo-neutrinos," *Physics Letters B*, vol. 687, no. 4-5, pp. 299–304, 2010.

[11] G. Bellini, J. Benziger, D. Bick et al., "Precision measurement of the ^{7}Be solar neutrino interaction rate in borexino," *Physical Review Letters*, vol. 107, Article ID 141302, 2011.

[12] K. Zuber, "Status of the double beta experiment COBRA," *Progress in Particle and Nuclear Physics*, vol. 57, pp. 235–240, 2006.

[13] M. Wurm, J. F. Beacom, L. B. Bezrukov et al., "The next-generation liquid-scintillator neutrino observatory LENA," *Astroparticle Physics*, vol. 35, no. 11, pp. 685–732, 2012.

[14] P. Zucchelli, "A novel concept for a $\bar{\nu}_e/\nu_e$ neutrino factory: the beta-beam," *Physics Letters B*, vol. 532, no. 3-4, pp. 166–172, 2002.

[15] C. Volpe, "What about a beta-beam facility for low-energy neutrinos?," *Journal of Physics G*, vol. 30, article L1, 2004.

[16] M. S. Athar and S. K. Singh, "$\nu_e(\bar{\nu}_e)$-^{40}Ar absorption cross sections for supernova neutrinos," *Physics Letters B*, vol. 591, no. 1-2, pp. 69–75, 2004.

[17] F. T. Avignone and Y. V. Efremenko, "ORLaND—a neutrino facility at the spallation neutron source," *Nuclear Physics B—Proceedings Supplements*, vol. 87, no. 1–3, pp. 304–308, 2000.

[18] F. T. Avignone III and Y. V. Efremenko, "Neutrino-nucleus cross-section measurements at intense, pulsed spallation sources," *Journal of Physics G: Nuclear and Particle Physics*, vol. 29, no. 11, pp. 2615–2628, 2003.

[19] R. L. Burman and W. C. Louis, "Neutrino physics at meson factories and spallation neutron sources," *Journal of Physics G*, vol. 29, no. 11, article 2499, 2003.

[20] E. Kolbe, K. Langanke, G. Martínez-Pinedo, and P. Vogel, "Neutrino–nucleus reactions and nuclear structure," *Journal of Physics G: Nuclear and Particle Physics*, vol. 29, no. 11, pp. 2569–2596, 2003.

[21] K. Langanke and G. Martinez-Pinedo, "Nuclear weak-interaction processes in stars," *Reviews of Modern Physics*, vol. 75, no. 3, pp. 819–862, 2003.

[22] A. Juodagalvis, K. Langanke, G. Martinez-Pinedo, W. R. Hix, D. J. Dean, and J. M. Sampaio, "Neutral-current neutrino–nucleus cross sections for A~50–65 nuclei," *Nuclear Physics A*, vol. 747, pp. 87–108, 2005.

[23] K. Langanke, "Weak interaction, nuclear physics and super-novae," *Acta Physica Polonica B*, vol. 39, no. 2, pp. 265–281, 2008.

[24] A. A. Aguilar-Arevalo, C. E. Anderson, A. O. Bazarko et al., "Search for core-collapse supernovae using the MiniBooNE neutrino detector," *Physical Review D*, vol. 81, Article ID 032001, 2010.

[25] H. Ejiri, J. Engel, and N. Kudomi, "Supernova-neutrino studies with ^{100}Mo," *Physics Letters Section B*, vol. 530, no. 1–4, pp. 27–32, 2002.

[26] W. C. Haxton, "Nuclear response of water Cherenkov detectors to supernova and solar neutrinos," *Physical Review D*, vol. 36, no. 8, pp. 2283–2292, 1987.

[27] S. W. Bruenn and W. C. Haxton, "Neutrino-nucleus interactions in core-collapse supernovae," *Astrophysical Journal Letters*, vol. 376, no. 2, pp. 678–700, 1991.

[28] V. Tsakstara and T. S. Kosmas, "Nuclear responses of ^{64,66}Zn isotopes to supernova neutrinos," *Physical Review C*, vol. 86, no. 4, Article ID 044618, 10 pages, 2012.

[29] V. Tsakstara and T. S. Kosmas, *Physical Review C*. To be submitted.

[30] K. G. Balasi, E. Ydrefors, and T. S. Kosmas, "Theoretical study of neutrino scattering off the stable even Mo isotopes at low and intermediate energies," *Nuclear Physics A*, vol. 868-869, no. 1, pp. 82–98, 2011.

[31] Y. Giomataris and J. D. Vergados, "A network of neutral current spherical TPCs for dedicated supernova detection," *Physics Letters B*, vol. 634, no. 1, pp. 23–29, 2006.

[32] J. D. Vergados and Y. Giomataris, "Dedicated supernova detection by a network of neutral current spherical TPC detectors," *Physics of Atomic Nuclei*, vol. 70, no. 1, pp. 140–149, 2007.

[33] J. D. Vergados, F. T. Avignone, and I. Giomataris, "Coherent neutral current neutrino-nucleus scattering at a spallation source: a valuable experimental probe," *Physical Review D*, vol. 79, no. 11, Article ID 113001, 2009.

[34] T. S. Kosmas, "Exotic $\mu^- \rightarrow e^-$ conversion in nuclei: energy moments of the transition strength and average energy of the outgoing e^-," *Nuclear Physics A*, vol. 683, no. 1–4, pp. 443–462, 2001.

[35] K. Zuber, "The status of the COBRA double-beta-decay experiment," *Progress in Particle and Nuclear Physics*, vol. 64, no. 2, pp. 267–269, 2010.

[36] J. N. Bachall and R. K. Ulrich, "Solar models, neutrino experiments, and helioseismology," *Reviews of Modern Physics*, vol. 60, p. 297, 1988.

[37] J. N. Bahcall, S. Basu, M. Pinsonneault, and A. M. Serenelli, "Helioseismological implications of recent solar abundance determinations," *The Astrophysical Journal*, vol. 618, no. 2, pp. 1049–1056, 2005.

[38] A. Gando, Y. Gando, K. Ichimura et al., "Partial radiogenic heat model for Earth revealed by geoneutrino measurements," *Nature Geoscience*, vol. 4, no. 9, pp. 647–651, 2011.

[39] G. Bellini, J. Benziger, D. Bick et al., "Measurement of geo-neutrinos from 1353 days of Borexino," *Physics Letters B*, vol. 722, no. 4-5, pp. 295–300, 2013.

[40] P. Vogel and J. F. Beacom, "Angular distribution of neutron inverse beta decay, $\bar{\nu}e + \vec{p}e^+ + \mathbf{n}$," *Physical Review D*, vol. 60, no. 5, Article ID 053003, 1999.

[41] S. Dye, "Geoneutrinos and the radioactive power of the Earth," *Reviews of Geophysics*, vol. 50, no. 3, Article ID RG3007, 2012.

[42] G. Fiorentini, F. Mantovani, and B. Ricci, "Neutrinos and energetics of the Earth," *Physics Letters B*, vol. 557, no. 3-4, pp. 139–146, 2003.

[43] G. Fiorentini, A. Ianni, G. Korga et al., "Nuclear physics for geo-neutrino studies," *Physical Review C*, vol. 81, no. 3, Article ID 034602, 9 pages, 2010.

[44] T. S. Kosmas, J. D. Vergados, O. Civitarese, and A. Faessler, "Study of the muon number violating (μ^-, e^-) conversion in a nucleus by using quasi-particle RPA," *Nuclear Physics, Section A*, vol. 570, no. 3-4, pp. 637–656, 1994.

[45] K. Abe, K. Abe, T. Abe et al., "Improved direct measurement of leptonic coupling asymmetries with polarized Z bosons," *Physical Review Letters*, vol. 86, no. 7, pp. 1162–1166, 2001.

[46] J. Engel, "Nuclear form factors for the scattering of weakly interacting massive particles," *Physics Letters B*, vol. 264, pp. 114–119, 1991.

[47] H. de Vries, C. W. de Jager, and C. de Vries, "Nuclear charge-density-distribution parameters from elastic electron scattering," *Atomic Data and Nuclear Data Tables*, vol. 36, no. 3, pp. 495–536, 1987.

[48] A. Drukier and L. Stodolsky, "Principles and applications of a neutral-current detector for neutrino physics and astronomy," *Physical Review D*, vol. 30, no. 11, article 2295, 1984.

[49] P. Vogel and J. Engel, "Neutrino electromagnetic form factors," *Physical Review D*, vol. 39, no. 11, pp. 3378–3383, 1989.

[50] J. D. Vergados, "Neutral current coherent cross sections-implications on gaseous spherical TPC's for detecting SN and Earth neutrinos," *Journal of Physics: Conference Series*, vol. 309, no. 1, Article ID 012031, 2011.

[51] T. W. Donnelly and J. D. Walecka, "Semi-leptonic weak and electromagnetic interactions in nuclei with application to 16O," *Physics Letters B*, vol. 41, no. 3, pp. 275–280, 1972.

[52] T. W. Donnelly and J. D. Walecka, "Elastic magnetic electron scattering and nuclear moments," *Nuclear Physics, Section A*, vol. 201, no. 1, pp. 81–106, 1973.

[53] E. Kolbe, "Differential cross sections for neutrino scattering on ^{12}C," *Physical Review C*, vol. 54, no. 4, pp. 1741–1748, 1996.

[54] D. K. Papoulias and T. S. Kosmas, "Nuclear aspects of neutral current non-standard ν-nucleus reactions and the role of the exotic $\mu^- \rightarrow e^-$ transitions experimental limits," *Physics Letters B*, vol. 728, pp. 482–488, 2014.

[55] A. de Gouvea, K. Pitts, K. Scholberg et al., "Neutrinos," http://arxiv.org/abs/1310.4340v1.

[56] B. R. Davis, P. Vogel, F. M. Mann, and R. E. Schenter, "Reactor antineutrino spectra and their application to antineutrino-induced reactions," *Physical Review C*, vol. 19, no. 6, pp. 2259–2266, 1979.

[57] Y. Declais, H. de Kerret, B. Lefièvre et al., "Study of reactor antineutrino interaction with proton at Bugey nuclear power plant," *Physics Letters B*, vol. 338, no. 2-3, pp. 383–389, 1994.

[58] O. Tengblad, K. Aleklett, R. von Dincklage, E. Lund, G. Nyman, and G. Rudstam, "Integral $\bar{\ }$ gn-spectra derived from experimental β-spectra of individual fission products," *Nuclear Physics A*, vol. 503, no. 1, pp. 136–160, 1989.

[59] W. C. Louis, "Searches for muon-to-electron (anti) neutrino flavor change," *Progress in Particle and Nuclear Physics*, vol. 63, pp. 51–73, 2009.

[60] E. Kolbe and T. S. Kosmas, "Recent highlights on neutrino-nucleus interactions," in *Symmetries in Intermediate and High Energy Physics*, vol. 163 of *Springer Tracts in Modern Physics*, pp. 199–225, Springer, 2000.

[61] T. S. Kosmas and J. D. Vergados, "Cold dark matter in SUSY theories: the role of nuclear form factors and the folding with the LSP velocity," *Physical Review D*, vol. 55, no. 4, pp. 1752–1764, 1997.

[62] V. Tsakstara, T. S. Kosmas, J. Sinatkas, V. C. Chasioti, and P. C. Divari, "The convolution method in neutrino physics searches," *AIP Conference Proceedings*, vol. 963, no. 2, p. 1383, 2007.

[63] V. A. Tsakstara, T. S. Kosmas, V. C. Chasioti, and J. Sinatkas, "On the nuclear response of ^{56}Fe to supernova neutrino spectra," in *Proceedings of the Carpathian Summer School of Physics (CSSP '07)*, vol. 972, pp. 562–565, Sinaia, Romania, August 2007.

[64] H. T. Janka and W. Hillebrand, "Neutrino emission from type II supernovae—an analysis of the spectra," *Astronomy & Astrophysics*, vol. 224, no. 1-2, pp. 49–56, 1989.

[65] M. T. Keil, G. G. Raffelt, and H.-T. Janka, "Monte Carlo study of supernova neutrino spectra formation," *The Astrophysical Journal*, vol. 590, no. 2, pp. 971–991, 2003.

[66] H. A. Bethe, "Supernova mechanisms," *Reviews of Modern Physics*, vol. 62, no. 4, pp. 801–866, 1990.

[67] C. Fröhlich, G. Martínez-Pinedo, M. Liebendörfer et al., "Neutrino-induced nucleosynthesis of A>64 nuclei: the νp process," *Physical Review Letters*, vol. 96, no. 14, Article ID 142502, 2006.

[68] H.-T. Janka and B. Müller, "Neutrino-driven type-II supernova explosions and the role of convection," *Physics Reports*, vol. 256, no. 1–3, pp. 135–156, 1995.

[69] H.-Th. Janka, K. Langanke, A. Mareka, G. Martinez-Pinedo, and B. Mullera, "Theory of core-collapse supernovae," *Physics Reports*, vol. 442, no. 1–6, pp. 38–74, 2007.

[70] B. Dasgupta and A. Dighe, "Collective three-flavor oscillations of supernova neutrinos," *Physical Review D*, vol. 77, Article ID 113002, 2008.

[71] G. G. Raffelt, M. T. Keil, R. Buras, H.-T. Janka, and M. Rampp, "Supernova neutrinos: flavor-dependent fluxes and spectra," http://arxiv.org/abs/astro-ph/0303226.

[72] V. Tsakstara and T. S. Kosmas, "Studying supernovae via their neutrino signatures at nuclear detectors," in *Horizons in World Physics*, vol. 278, chapter 7, pp. 219–254, Nova Science Publishers, 2012.

[73] V. Tsakstara, T. S. Kosmas, P. C. Divari, and J. Sinatkas, "The interpretation of SN–ν signals in terrestrial experiments through the folding procedure," *AIP Conference Proceedings*, vol. 1180, pp. 140–144, 2009.

[74] V. Tsakstara and T. S. Kosmas, "Neutrino-nucleus reactions in terrestrial experiments and astrophysics," *Progress in Particle and Nuclear Physics*, vol. 64, no. 2, pp. 407–410, 2010.

[75] N. Jachowicz and G. C. McLaughlin, "Reconstructing supernova-neutrino spectra using low-energy beta beams," *Physical Review Letters*, vol. 96, Article ID 172301, 2006.

[76] N. Jachowicz, G. McLaughlin, and C. Volpe, "Untangling supernova-neutrino oscillations with β-beam data," *Physical Review C*, vol. 77, no. 5, Article ID 055501, 12 pages, 2008.

[77] C. Volpe, "Beta-beams," *Journal of Physics G: Nuclear and Particle Physics*, vol. 34, no. 1, pp. R1–R44, 2007.

[78] V. Tsakstara, T. S. Kosmas, and J. D. Vergados, "Weak responses of neutral current neutrino-nucleus," *Romanian Journal of Physics*, vol. 58, no. 9-10, pp. 1258–1269, 2013.

Journal of
Gravity

Journal of
Photonics

The Scientific World Journal

Journal of
Soft Matter

Advances in
Condensed Matter Physics

Journal of
Fluids

Journal of
Aerodynamics

International Journal of
Statistical Mechanics
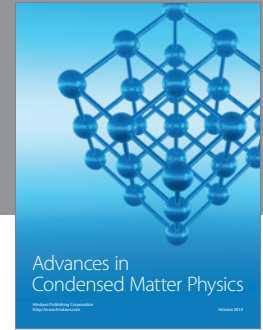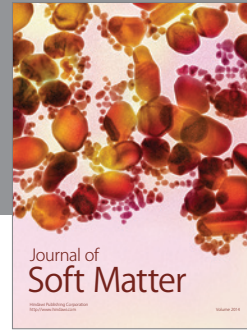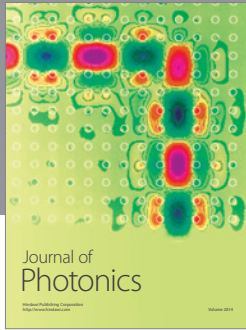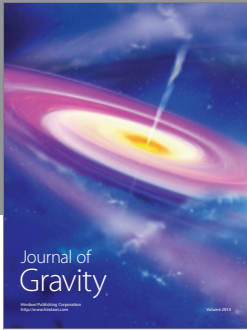
![Hindawi]

Submit your manuscripts at
http://www.hindawi.com

International Journal of
Optics

Journal of
Computational Methods in Physics

Advances in
High Energy Physics

Journal of
Thermodynamics

Physics Research International

Advances in
Astronomy

Journal of
Solid State Physics

Journal of
Astrophysics

International Journal of
Superconductivity

Journal of
Biophysics

Journal of
Atomic and Molecular Physics